Journal of Physics: Conference Series **1643** (2020) 012084 doi:10.1088/1742-6596/1643/1/012084

Nucleus-nucleus potentials from local chiral EFT interactions

V. Durant[1], P. Capel[1,2], A. Schwenk[3,4,5]

[1] Institut für Kernphysik, Johannes Gutenberg-Universität Mainz, D-55099 Mainz, Germany
[2] Physique Nucléaire et Physique Quantique (CP 229),Université libre de Bruxelles (ULB), B-1050 Brussels, Belgium
[3] Institut für Kernphysik, Technische Universität Darmstadt, 64289 Darmstadt, Germany
[4] ExtreMe Matter Institute EMMI, GSI Helmholtzzentrum für Schwerionenforschung GmbH, 64291 Darmstadt, Germany
[5] Max-Planck-Institut für Kernphysik, Saupfercheckweg 1, 69117 Heidelberg, Germany

E-mail: vdurant@uni-mainz.de

Abstract. We present the first determination of double-folding potentials (DFP) based on chiral effective field theory (EFT) nucleon-nucleon interactions at next-to-next-to-leading order (N^2LO). To this end, we construct new two-body soft local chiral EFT interactions. We benchmark this approach in ^{16}O-^{16}O collisions, and extend it to the scattering of ^{12}C-^{12}C. We present results for cross sections computed for elastic scattering at energies up to 1000 MeV, as well as for the astrophysical S factor of the fusion of oxygen isotopes. Thanks to the predictive power of this approach, we can calculate various reaction observables without any adjusting parameters. Our analysis of these various reaction observables has enabled us to study the impact of the nuclear density and the nucleon-nucleon interaction on the corresponding cross sections.

1. Introduction

Nuclear reactions are widely used to, e.g., obtain information about nuclear structure far from stability or study astrophysical phenomena. In order to analyse data or obtain theoretical predictions for reaction observables, important inputs are potentials that simulate the interaction between the colliding nuclei [1]. Historically, these potentials were fitted from data for each pair of colliding nuclei and energy. Therefore, they are precise when experimental data exists, but lack predictive power.

In recent years, there has been encouraging progress on ab initio reaction description, especially for nucleon-nucleus scattering, applying many-body perturbation theory or self-consistent Green's function calculations, for example. To describe nucleus-nucleus scattering, double-folding potentials (DFP), constructed from the densities of the colliding nuclei and a given nucleon-nucleon (NN) interaction, provide potentials relevant in the modelling of reactions used to infer nuclear-structure information or reaction rates of astrophysical interest

In this formalism, the antisymmetrized DFP, $V_{\rm F}$, can be obtained by integrating the NN interaction over the densities in the direct (D) channel and the density matrices in the exchange (Ex) channel. The expressions for these potentials can be found in Sec. II of Ref. [2, 3].

In our work, we use two-parameter Fermi distributions for the proton and neutron densities. We adopt the fits performed by the São Paulo group [4]. Furthermore, to study the impact of the chosen density, we also consider realistic density profiles, coming from electron-scattering or mean-field calculations, specific for the nuclei of interest in the following sections.

Because it simplifies the double-folding procedure, we use the coordinate-space representation of local chiral NN interactions, developed initially in Refs. [5, 6, 7]. In this prescription, the long- and short-range parts of the interaction are regularized by

$$f_{\rm long}(r) = 1 - e^{-(r/R_0)^4} \text{ and } f_{\rm short}(r) = \frac{e^{-(r/R_0)^4}}{\pi\Gamma(3/4)R_0^3}\,, \tag{1}$$

where R_0 is the coordinate-space cutoff in the NN potentials used. The long-range regulator is designed to remove the singularity at $r = 0$ in the pion exchanges, while it preserves its properties at large distances. The short-range regulator smears out the NN contact interactions.

To perform the calculations of DFP, we use the NN interactions with $R_0 = 1, 2, 1.4$ and 1.6 fm developed in Ref. [3]. All results shown in this work are calculated at N^{2}LO. For a discussion of the order-by-order behavior of the double-folding potential and reaction observables, we refer the reader to Ref. [3].

2. Elastic scattering

To describe elastic scattering of nuclei, we apply the optical model. In order to model non-elastic channels that can be open during the collision, the nuclear part of the nucleus-nucleus interaction has an imaginary part. In this first study, the real part of the optical potential is composed of the DFP, and we follow the São Paulo group and assume the imaginary part of the optical potential $U_{\rm F}$ to be proportional to its real part [8]

$$U_{\rm F}(r, E) = (1 + i\,N_W)\,V_{\rm F}(r, E)\,, \tag{2}$$

where $V_{\rm F}$ is our DFP, obtained without any fitting parameter, E is the energy of the collision, and N_W is a real coefficient taken in the range 0.6–0.8.

2.1. ^{16}O–^{16}O

The elastic scattering cross sections computed at laboratory energies between 124 and 704 MeV are displayed in Fig. 1 as a ratio to the Mott cross section. The bands are delimited by results obtained for the range $N_W = 0.6 - 0.8$. In general, we observe good agreement between our calculations and the data, especially at forward angles. At a larger momentum transfer, the agreement is less good, although the spread obtained for the N_W range remains close to the experimental points. This shows that going beyond the simple description of the imaginary part could improve our calculations.

The left panel of Fig. 1 shows results generated by the cutoffs $R_0 = 1.2$ fm, 1.4 fm, and 1.6 fm displayed in red, blue, and green, respectively. We find that the cutoff variation is less relevant than the impact of the imaginary part coefficient N_W. The right panel shows results for $R_0 = 1.4$ fm obtained with a two-parameter Fermi density (blue band) and with two density distributions parametrized from electron-scattering experiments on ^{16}O (green and magenta bands). The two densities electron-scattering data lead to almost indistinguishable cross sections. It is clear from the figure that the impact of the chosen density profile is smaller than the impact of the imaginary part, confirming the need to better constrain this part of the potential.

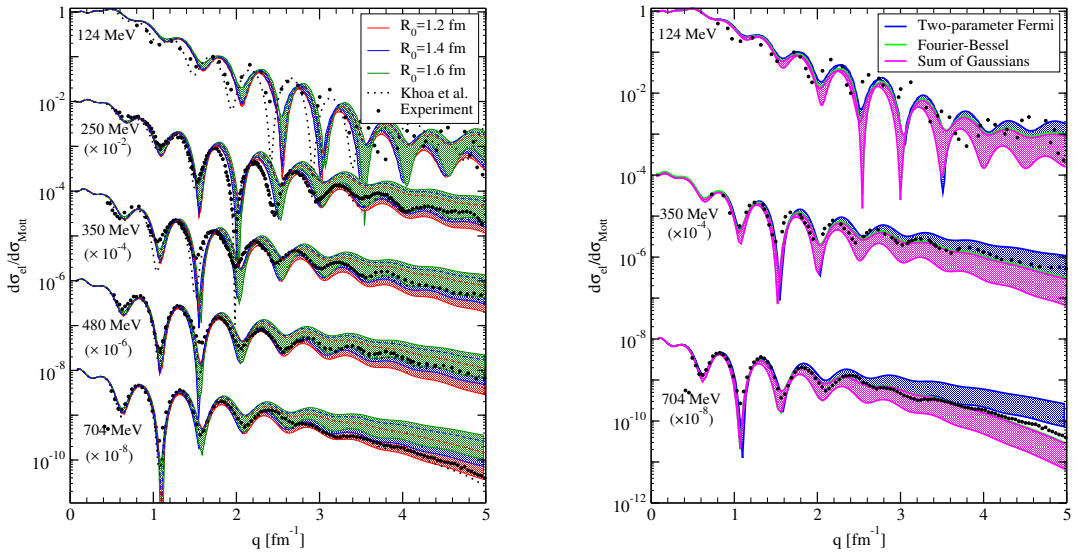

Figure 1. Elastic-scattering cross section for ^{16}O–^{16}O (ratio to the Mott cross section) as a function of momentum transfer q for various laboratory energies. For all results the shaded areas delimit calculations with $N_W = 0.6$ and $N_W = 0.8$. The optical-potential results of Khoa *et al.* are shown for comparison, as well as existing experimental data, see Ref. [9].
Left: Results obtained with a two-parameter Fermi distribution [4] for $R_0 = 1.2$ fm (red), 1.4 fm (blue), and 1.6 fm (green).
Right: Results for $R_0 = 1.4$ fm using different density distributions: two-parameter Fermi [4] (blue) and Fourier-Bessel (green) and Sum of Gaussians (orange) parametrisations obtained from electron-scattering [10].

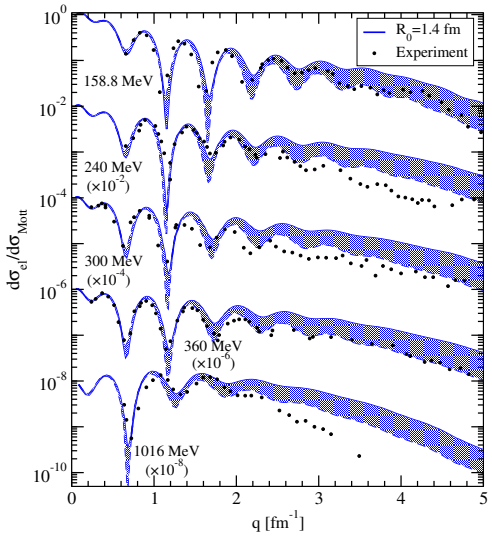

Figure 2. Ratio of the cross section for elastic ^{12}C–^{12}C scattering to the Mott cross section as a function of momentum transfer q for various laboratory energies. The region between the results with $N_W = 0.6$ and $N_W = 0.8$ is shaded.

2.2. ^{12}C–^{12}C

We have extended this formalism to the case of ^{12}C–^{12}C elastic scattering. The corresponding cross sections can be found in Fig. 2. The bands are calculated for $R_0 = 1.4$ fm and are delimited by results for the range $N_W = 0.6 - 0.8$. The reproduction of experimental data [11, 12, 13, 14] is comparable to the case of ^{16}O–^{16}O for forward angles at all the energies explored. At large momentum transfers this comparison is less good than that for ^{16}O–^{16}O, but the impact of N_W is also enhanced, which further reinforces the need of a refined description of the imaginary part of the optical potential.

3. Fusion reactions

Oxygen fusion is crucial in medium-mass nuclei burning chains, especially in the case of 8–12 $M_\odot$ stars, where ^{20}O can be produced via electron capture on ^{20}Ne [15, 16]. Given its presence in medium-mass stars, we study the fusion of ^{16}O+^{16}O, ^{16}O+^{20}O, and ^{20}O+^{20}O using our DFP.

In the case of nuclear fusion involving collisions of light to medium-mass nuclei at astrophysical energies, one can usually assume that the effective potential is formed by the real part of the nuclear interaction [17] and the Coulomb potential between the nuclei. For light systems like oxygen, the fusion barrier is situated well before the neck formation, which justifies the use of the double-folding procedure. The fusion cross sections are determined using the code CCFULL [18], in which we have included the effects of the symmetrization of the wave function needed in the case in which the fusing nuclei are spinless bosons.

At low energy, the fusion process is strongly hindered by the Coulomb repulsion, which makes the cross sections drop rapidly when the center-of-mass energy, $E_{\rm cm}$, decreases. This hindrance of the fusion process is well accounted for by the Gamow factor, which is usually factorized out of the cross section to define the astrophysical S factor

$$S(E_{\rm cm}) = E_{\rm cm}\, e^{2\pi\eta}\, \sigma_{\rm fus}(E_{\rm cm})\,, \tag{3}$$

where η is the Sommerfeld parameter.

We perform the calculation of the DFP for ^{16}O–^{16}O using density profiles from two-parameter Fermi distributions and parametrizations of electron-scattering experiments [10] to assess the impact of the nuclear density on the fusion cross section. The left panel of Fig. 3 shows the S factor as a function of the center-of-mass energy. Results using these realistic densities can be seen in magenta, while those obtained from two-parameter Fermi distributions are shown in blue. The shaded bands are delimited by the variation $R_0 = 1.4$–1.6 fm. From this comparison, it is clear that the nuclear density plays an important role in the fusion cross section, and that it is larger than the sensitivity to the details of the NN interaction. It is also clear that the use of realistic densities is crucial for the reproduction of experimental data, shown as black symbols (see [3] for a list of references).

The right panel of Fig. 3 shows a summary of the S factors for ^{16}O+^{16}O, ^{16}O+^{20}O, and ^{20}O+^{20}O as a function of the center-of-mass energy. The magenta band for ^{16}O+^{16}O corresponds to the result shown in the left panel. In these calculations, we use the ^{16}O density derived from electron elastic-scattering and the result of a Hartree-Fock-Bogoliubov (HFB) calculation [19] for ^{20}O. The parametrisations of Refs. [20, 21] are shown as black lines. For these three systems, the S factors resulting from DFP using chiral EFT NN interactions calculated with realistic densities confirm the validity of the aforementioned theoretical predictions [20, 21] in the whole range of energies of astrophysical interest.

4. Summary and conclusions

We have presented nucleus-nucleus potentials from local chiral NN interactions [5, 6, 7] with a soft cutoff [3] using the double-folding method applied to elastic scattering of ^{16}O–^{16}O and

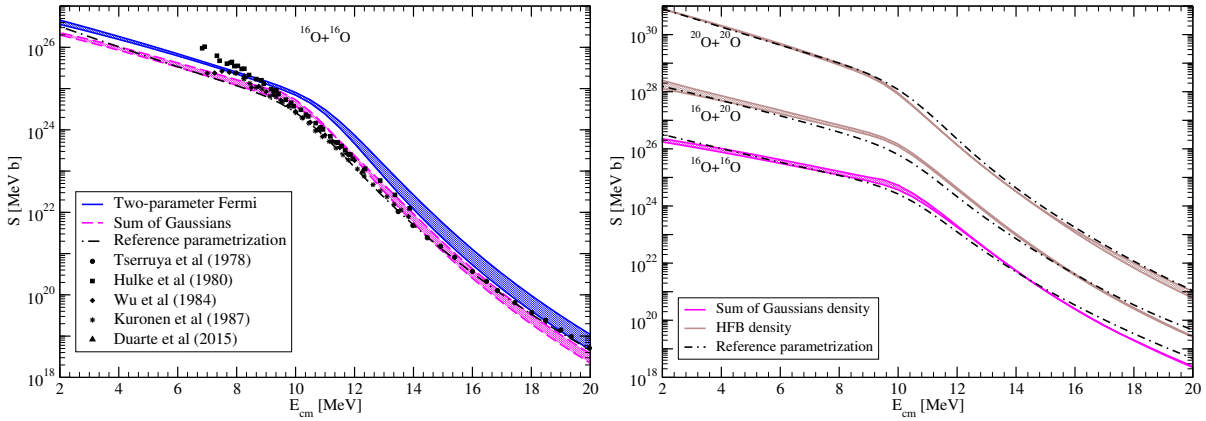

Figure 3. Astrophysical S factor for the fusion of oxygen isotopes as a function of the energy $E_{\rm cm}$ in the center-of-mass system. The shaded area illustrates the sensitivity to $R_0 = 1.2$–1.6 fm. Left: Results for ^{16}O+^{16}O fusion obtained using a two-parameter Fermi distribution (blue band) and densities obtained from electron-scattering (orange band).
Right: Fusion of ^{16}O+^{16}O, ^{16}O+^{20}O, and ^{20}O+^{20}O. For all systems, the nuclear potential was calculated with realistic density profiles. The black line shows the results of the parametrisations of Refs. [20, 21].

^{12}C–^{12}C, and the fusion involving oxygen isotopes. In all cases, we obtain good agreement with experimental data and/or existing theoretical results without the need of any fitting parameter.

We find that to accurately describe elastic scattering we need to refine the description imaginary part of the potential. Assuming it to be proportional to the double-folding potential provides a first estimate that validates this approach, but it is clear that this can be improved. Possible paths to achieve this are calculations beyond Hartree-Fock [22, 23], going further in density-matrix expansion considered here [24], or the application of dispersion relations [25].

Our studies show that the choice of density to describe the reacting nuclei has a significant impact in the fusion observables, namely the S factor, contrary to what is seen in elastic-scattering calculations, where the influence is small. In particular, in order to accurately reproduce data, we need to consider realistic densities to construct the double-folding potentials.

In conclusion, these results confirm that coupling chiral EFT interactions with the double-folding method provides nucleus-nucleus potentials is a promising path towards the description of reactions from first principles. Through the aforementioned future developments, we hope to improve this new method to obtain a systematic way to build efficient optical potentials for nuclear reactions.

Acknowledgments

We thank L. Huth for the fits of the potentials with $R_0 = 1.4$ and 1.6 fm, B. Balantekin for interesting ideas and discussions, and E. Khan for providing density profiles from his HFB calculations. We also thank the International Atomic Energy Agency that provided the experimental data through their web page www-nds.iaea.org. This work is supported by the PRISMA+ (Precision Physics, Fundamental Interactions and Structure of Matter) Cluster of Excellence, the European Union's Horizon 2020 research and innovation programme under Grant Agreement No. 654002, and the Deutsche Forschungsgemeinschaft within the Collaborative Research Centers 1245 and 1044.

References

[1] Brandan M and Satchler G 1997 *Phys. Rep.* **285** 143
[2] Furumoto T, Horiuchi W, Takashina M, Yamamoto Y and Sakuragi Y 2012 *Phys. Rev. C* **85** 044607
[3] Durant V, Capel P, Huth L, Balantekin A B and Schwenk A 2018 *Phys. Lett. B* **782** 668
[4] Chamon L C, Carlson B V, Gasques L R, Pereira D, De Conti C, Alvarez M A G, Hussein M S, Candido Ribeiro M A, Rossi Jr E S and Silva C P 2002 *Phys. Rev. C* **66** 014610
[5] Gezerlis A, Tews I, Epelbaum E, Gandolfi S, Hebeler K, Nogga A and Schwenk A 2013 *Phys. Rev. Lett.* **111** 032501
[6] Gezerlis A, Tews I, Epelbaum E, Freunek M, Gandolfi S, Hebeler K, Nogga A and Schwenk A 2014 *Phys. Rev. C* **90** 054323
[7] Huth L, Tews I, Lynn J E and Schwenk A 2017 *Phys. Rev. C* **96** 054003
[8] Pereira D, Lubian J, Oliveira J R B, de Sousa D P and Chamon L C 2009 *Phys. Lett. B* **670** 330
[9] Khoa D T, von Oertzen W, Bohlen H G and Nuoffer F 2000 *Nucl. Phys. A* **672** 387
[10] Vries H D, Jager C D and Vries C D 1987 *Atomic Data and Nuclear Data Tables* **36** 495
[11] Kubono S, Morita K, Tanaka M H, Sugitani M, Utsunomiya H and Yonehara H 1983 *Phys. Lett. B* **127** 19
[12] Bohlen H G, Clover M R, Ingold G, Lettau H and von Oertzen W 1982 *"Zeitschrift für Physik A Atoms and Nuclei"* **308** 121
[13] Buenerd M, Pinston J, Cole J, Guet C, Lebrun D, Loiseaux J, Martin P, Monnand E, Mougey J, Nifenecker H *et al.* 1981 *Physics Letters B* **102** 242
[14] Buenerd M, Lounis A, Chauvin J, Lebrun D, Martin P, Duhamel G, Gondrand J and Saintignon P D 1984 *Nuclear Physics A* **424** 313
[15] Nomoto K 1983 *Astrophys. J.* **277** 791
[16] Nomoto K 1987 *Astrophys. J.* **322** 206
[17] Hagino K and Takigawa N 2012 *Prog. Theor. Phys.* **128** 1061
[18] Hagino K, Rowley N and Kruppa A T 1999 *Comput. Phys. Commun.* **123** 143
[19] Khan E *et al.* 2000 *Phys. Lett. B* **490** 45
[20] Gasques L R, Afanasjev A V, Beard M, Lubian J, Neff T, Wiescher M and Yakovlev D G 2007 *Phys. Rev. C* **76** 045802
[21] Beard M, Afanasjev A V, Chamon L C, Gasques L R, Wiescher M and Yakovlev D G 2010 *Atom. Data Nucl. Data Tabl.* **96** 541
[22] Feshbach H 1958 *Ann. Phys.* **5** 357
[23] Feshbach H 1962 *Ann. Phys.* **19** 287
[24] Negele J W and Vautherin D 1972 *Phys. Rev. C* **5** 1472
[25] Carlson R V, Frederico T, Hussein M S, Esbensen H and Landowne S 1989 *IFUSP/P-802 (1989)*